Colossal C_{130} Fullertubes: Soluble [5,5] C_{130}-D_{5h}(1) Pristine Molecules With 70 Nanotube Carbons And Two 30-Atom Hemifullerene Endcaps

Emmanuel Bourret,[1] Xiaoyang Liu,[2] Cora A. Noble,[3] Kevin Cover,[2] Tanisha P. Davidson,[3,5] Rong Huang,[2] Ryan M. Koenig,[3] K. Shawn Reeves,[4] Ivan V. Vlassiouk,[4] Michel Côté,[1] Jefferey S. Baxter,[4] Andrew R. Lupini,[4,*] David B. Geohegan,[4,*] Harry C. Dorn[2,*] and Steven Stevenson[3,5*]

1. Département de Physique, Université de Montréal, Montréal, H2V 0B3, Canada

2. Department of Chemistry, Virginia Tech, Blacksburg, VA 24061, United States

3. Department of Chemistry and Biochemistry, Purdue University Fort Wayne, Fort Wayne, IN 46805, United States

4. Center for Nanophase Materials Sciences Oak Ridge National Laboratory, Oak Ridge, TN 37831, United States

5. FIRST Molecules Center, Purdue University Fort Wayne, Fort Wayne, IN 46805, United States

KEYWORDS. Fullertubes, Nanotubular Fullerenes, Nanotubes, SWCNTs, Fullerenes, Anisotropic Polarizability, TEM

ABSTRACT: We report the seminal experimental isolation and DFT characterization of pristine [5,5] C_{130}-D_{5h}(1) fullertubes. This achievement represents the largest soluble carbon molecule obtained in pristine form. The [5,5] C_{130} species is the highest aspect ratio fullertube purified to date and now surpasses the recent gigantic [5,5] C_{120}-D_{5d}(1). In contrast to C_{90}, C_{100}, and C_{120} fullertubes, the longer C_{130}-D_{5h} has *more* nanotubular carbons (70) than end-cap fullerenyl atoms (60). Starting from 39,393 possible C_{130} isolated pentagon rule (IPR) structures and after analyzing polarizability, retention time, and UV-vis spectra, these three layers of data remarkably predict a single candidate isomer and fullertube, [5,5] C_{130}-D_{5h}(1). This structural assignment is augmented by atomic resolution STEM data showing distinctive and tubular "pill-like" structures with diameters and aspect ratios consistent with [5,5] C_{130}-D_{5h}(1) fullertubes. The high selectivity of the aminopropanol reaction with spheroidal fullerenes permits a facile separation and removal of fullertubes from soot extracts. Experimental analyses (HPLC retention time, UV-vis, and STEM) were synergistically used (with polarizability and DFT property calculations) to down select and confirm the C_{130} fullertube structure. Achieving the isolation of a new [5,5] C_{130}-D_{5h} fullertube opens the door to application development and fundamental studies of electron confinement, fluorescence, and metallic character for a fullertube series of molecules with systematic tubular elongation. This [5,5] fullertube family also invites comparative studies with single-walled carbon nanotubes (SWCNTs), nanohorns (SWCNHs), and fullerenes.

In the 1990s, Harigaya[1] envisioned a segmental family of [5,5] fullertubes (Fig. 1a). Beginning with C_{90}-D_{5h}(1), this *predicted* but not *experimentally* proven *family* of "in-between" molecules is defined by nanotubular carbons with hemispherical fullerene endcaps. Now, several questions emerge. At what length do fullertubes behave as a nanotubes? Are fullertubes classified as (a) nanotubes, (b) fullerenes, or (c) neither (*i.e.*, unique chemical, catalytic, and electronic properties)?

C_{60} and C_{70} fullerenes were purified 33 years ago (Fig. 1a).[2] Two decades later, a C_{90} fullertube was reported in 2010.[3] Ten years later, Stevenson[4] (2020) isolated pristine [5,5] C_{100}-D_{5d}(1) fullertube via chemical separation. In 2021, metallic predictions were discussed for [5,5] C_{90}-D_{5h}(1) and the longer [5,5] C_{100}-D_{5d}(1) fullertube.[5] In 2022, Dorn and Stevenson reported pristine metallic [5,5] C_{120}-D_{5d}(1) and non-metallic [10,0] C_{120}-D_{5d}(10766) fullertubes.[6] Recently, Otero and coworkers[7] conducted computational and adsorption studies for [5,5] C_{90}-D_{5h} fullertubes onto Ag(111) and Au(111) surfaces. Therein, [5,5] C_{90}-D_{5h} molecular orbitals were classified as nanotube like (*i.e.*, arising from quantum confinement of delocalized CNT bands) versus fullerene-like (*i.e.*, arising from the endcaps).[7]

For application development, Echegoyen and Sreenivasan (2022) found high catalytic activity for C_{96} fullertube in oxygen reduction reactions.[8] In parallel, Guldi (2022) reported C_{100}-D_{5d}(1) fluorescence.[9] Transient absorption spectroscopy indicated photoexcited C_{100}-D_{5d}(1) fullertube exhibits a slow intersystem crossing to generate a triplet excited state.[9]

This outburst of fullertube discoveries from 2020-2022 used only *micrograms*, rather than milligram quantities required for X-ray crystallography and ^{13}C NMR. Our breakthrough for fullertube isolation was the chemical selectivity of aminopropanol to separate tubular carbon versus spherical fullerenes[4-6]

Earlier C_{120} isomers matched *two* isolated unknowns from a pool of fullertube candidates, *i.e.*, [5,5] C_{120}-D_{5d}(1) and [10,0] C_{120}-D_{5h}(10766).[6] Serendipitously for C_{130}, there is *one* possible *tubular* high symmetry isomer, *i.e.*, a [5,5] C_{130}-D_{5h}(1) fullertube (Fig. 1c). Herein, we progress from a hypothesis of a single C_{130} candidate fullertube, to its isolation, seminal experimental characterization, and conclude with atomic resolution

TEM to confirm our original hypothesis of having purified a new molecule, a [5,5]C_{130}-D_{5h}(1) fullertube.

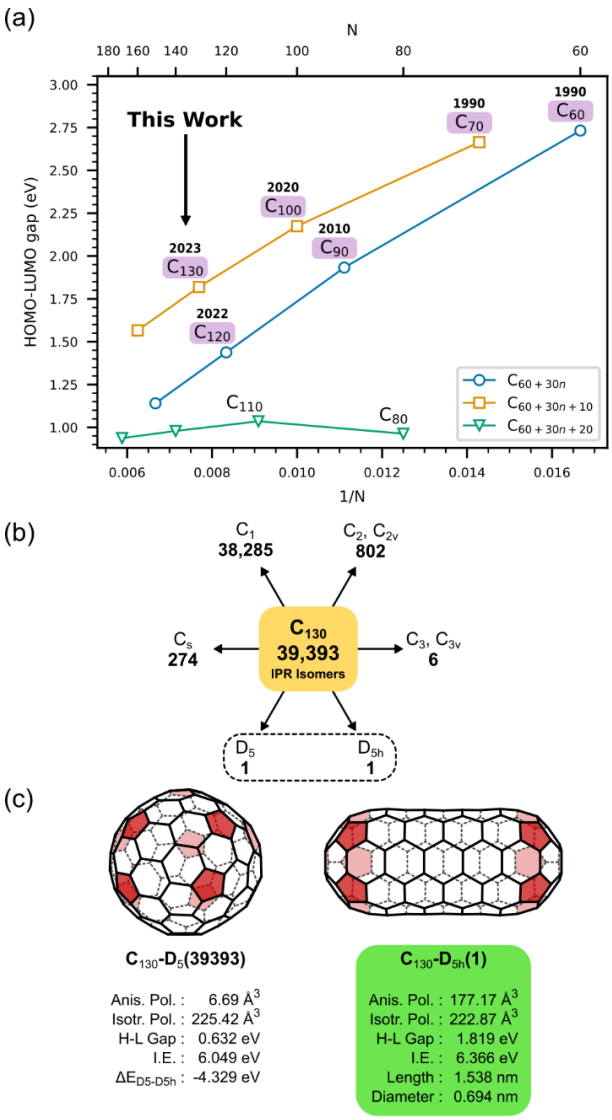

Figure 1. (a) HOMO-LUMO plot for the three series of [5,5] fullertubes (i.e., fullertubes begin with it smallest member, C_{90}), (b) number of IPR structures, and (c) DFT calculated values for anisotropic and isotropic polarizability, HOMO-LUMO gap, ionization energy, and energy gap for D_5 and D_{5h} isomers.

Our C_{130} journey begins with the down selection of 39,393 IPR (isolated pentagon rule)[10] structural isomers (Fig. 1b). Over twenty years ago, Cioslowski and coworkers[11] predicted that [5,5] and [9,0] endcapped nanotubes (fullertubes) can be described as appropriate models for single-walled carbon nanotubes (SWNTs). Consistent with their predictions, [5,5] C_{90} -D_{5h}, [5,5] C_{100}-D_{5d}, [5,5] C_{120}-D_{5d} and now [5,5] C_{130}-D_{5h} [5,5] have endcaps derived from C_{60}-I_h hemispheres.[4-6] The only other fullertubes isolated to date, (C_{96}-D_{3d}, and C_{120}-D_{5h}) have commonly recognized high symmetry endcaps.[4,6] With this criteria, we limited DFT computations to 3, 5, and 6 fold IPR allowed symmetry isomers for C_{130} (Fig. 1b). The eight C_3, C_{3v}, D_5 and D_{5h} IPR structural isomers of C_{130} are shown in the SI along with relevant DFT calculated properties.

As illustrated in Fig. 1b, there are six 3-fold and two 5-fold isomers. The C_3 and C_{3v} isomers are not possible fullertubes due to their different endcaps and structural features. Nevertheless, we included these six C_3 and C_{3v} structures and computed their properties (polarizability, HOMO-LUMO gap) for comparison (see SI). We are left with only the two structural candidates shown in Fig 1c. One structure is a spherical isomer (D_5). Likewise, there is one fullertube isomer, [5,5] C_{130}-D_{5h}(1). A side-by-side comparison of their DFT characteristics is shown in Fig. 1c. Also note in Fig. 1a that the C_{130}-D_{5h}(1) fullertube, with its longer aspect ratio, actually has a *larger* DFT predicted HOMO-LUMO gap (1.819 eV) than the previously reported[6] smaller [5,5] C_{120}-D_{5d}(1) fullertube (1.454 eV).

The first *experimental* stage for isolating C_{130} uses a selective reaction with aminopropanol to chemically separate *spheroidal* fullerenes (C_{76}-C_{200}) as water soluble derivatives.[4-6] Unreactive tubular carbon (fullertubes) remain in the organic layer for subsequent separation in a separatory funnel (see SI). Total isomeric resolution of C_{130} fullertubes was achieved using a PYE (pyrenyl-ethyl) stationary phase. Repeated HPLC injection and fraction collection was performed for C_{130} (see SI). Eventually, a mass spectrum (Fig. 2a) corresponding to a single chromatographic peak was achieved at 47.4 min for C_{130} (Fig. 2c). Final purified samples were monitored by *online* HPLC-UV-vis detection. Multiple UV-vis spectra (from a PDA detector) were taken across the HPLC peak profile (front, mid, and tail region). As shown in Fig. 2b, the pre-and post-UV-vis spectra are similar to the final collected UV-vis spectrum. The yield of purified C_{130} fullertube was ~50 micrograms, an amount suitable for TEM investigations but not amenable to X-ray crystallography or ^{13}C NMR.

Our first layer of structural support compares the UV-vis from DFT calculations versus the experimentally isolated C_{130} spectrum. As shown in the **SI**, there is remarkable agreement between the experimental UV-vis (685 nm, max.) and the DFT UV-vis (685.8, max.) spectrum for the [5,5] C_{130}-D_{5h}(1) isomer. This UV-vis spectrum was our first experimental data suggesting the isolation of [5,5] C_{130}-D_{5h}(1) fullertube. As shown in Fig. 3, a spectral comparison for the C_{90}, C_{100}, C_{120}, and C_{130} fullertube family indicates a progressive red shift in order of increasing [5,5] length from C_{90} to C_{130}.

Guldi and coworkers[9] experimentally addressed the optical bandgap for the case of [5,5] C_{90} -D_{5h} and [5,5] C_{100}-D_{5d} and found that the optical bandgap actually increases in progressing from [5,5] C_{90} -D_{5h} to [5,5] C_{100} -D_{5d} (Table 1). In contrast to nonluminescent [5,5] C_{90} -D_{5h}, [5,5], C_{100}-D_{5d} luminesces.[9] However, there is an oscillatory bandgap decrease in progressing from [5,5] C_{90} -D_{5h} to [5,5] C_{120} -D_{5d}. This was also predicted by Harigaya[1] (see Fig. 1) and Cioslowski.[11]

There is consistency with the observed color (Fig. 3e) and color complements for the UV-vis (max.) peaks for C_{90}-D_{5h}(1) and C_{100}-D_{5h}(1). However, the increasing red shift for the dominant peaks of C_{120}-D_{5h}(1) and C_{130}-D_{5h}(1) leads to lower spectral intensity in the spectral region (400-600 nm). An important

point of emphasis is the solubility of the entire [5,5] C_{90} to [5,5] C_{130} fullertube family in carbon disulfide and aromatic hydrocarbon solvents.

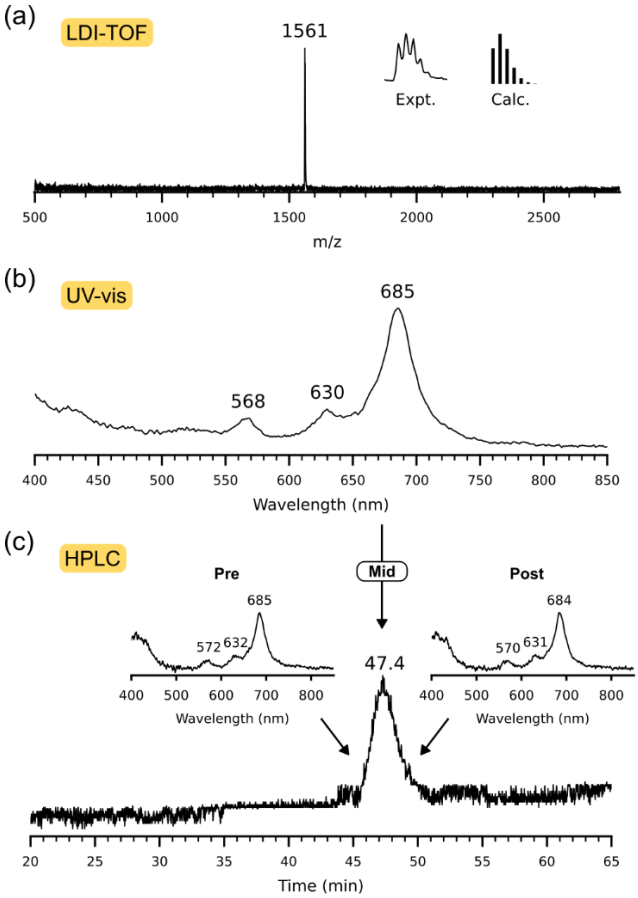

Figure 2. Characterization of purified [5,5] C_{130}-D_{5h}(1) fullertube via (a) LDI-TOF mass spectrometry, (b) UV-vis spectrum in o-xylene, and (c) Chromatogram with on-line HPLC-PDA spectra for front, mid, and back regions of the peak. HPLC conditions: 10 mm x 250 mm PYE column, 3.06 mL/min o-xylene mobile phase, 3000 μL injection, and 685 nm detection.

A second experimental layer of structural support compares DFT polarizability with experimental retention time. As shown in Fig. 4, the chromatographic ln *k* retention factor is plotted against either isotropic (Fig. 4a) or anisotropic (Fig. 4b) polarizability. If one assumes an *a priori* lack of knowledge of the C_{130} sample chromatographic retention time (correlation without the C_{130} data point in Fig. 4a), then the predicted value is 213.02 Å³ (4.4% difference). Incorporation of the C_{130} data point predicts a value of 218.71 Å³ (1.9% difference). Both of these numbers are reasonably close to the DFT predicted polarizability of 222.87 Å³ shown in Fig. 1c.

Plots of polarizability versus chromatographic retention are utilized in prior studies[12] for spherical and ellipsoidal molecules and could also be useful for distinguishing between even larger spherical and ellipsoidal fullerenes (C_{130}-C_{200}). For direct comparison with prior work on [5,5] C_{120}-D_{5d}(1) and [10,0] C_{120}-D_{5d}(10766),[6] anisotropic polarizability was plotted versus ln t_r/t_o retention time data (see SI.)

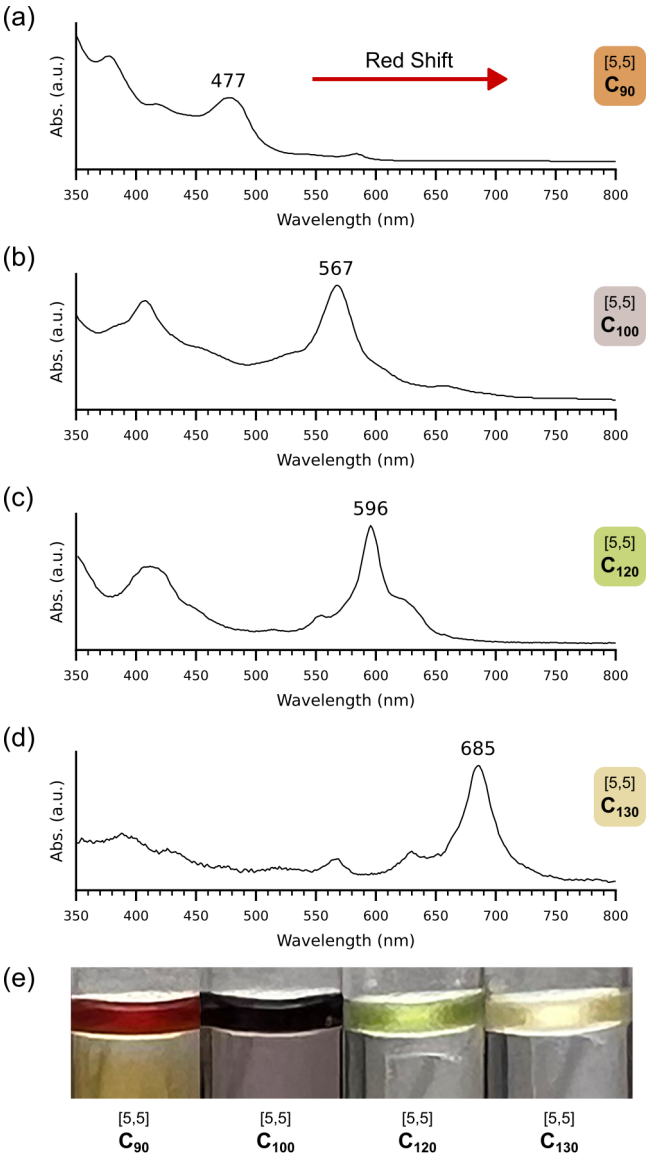

Figure 3. UV-vis spectra of purified (a) C_{90} -D_{5h}, (b) C_{100}-D_{5d}, (c) C_{120}-D_{5d}, (d) C_{130}-D_{5h} [5,5] fullertube family members. Spectra were obtained in o-xylene mobile phase with online PDA detection, (e) [5,5] fullertube samples (dissolved in CS_2) in 5 mm NMR tubes, with the picture taken at the meniscus.

Putting into context the achievement of isolating a soluble molecule with 130 carbon atoms, note that during the 30 year period from 1990-2020, the narrative among scientists was the Herculean task it would be to isolate, much less characterize, *any* isomerically purified samples for *any* structure above C_{100}. To do so, one would need to overcome the increasing number of candidate IPR isomers that, if formed, would represent an enormous separation problem of numerous co-eluting HPLC

peaks. Moreover, HOMO-LUMO gaps for larger carbon structures were predicted to further decrease, thereby lowering isomer stability. Further, it was suggested that the higher fullerene isomers greater than C_{100} would have little to no solubility in common aromatic solvents.

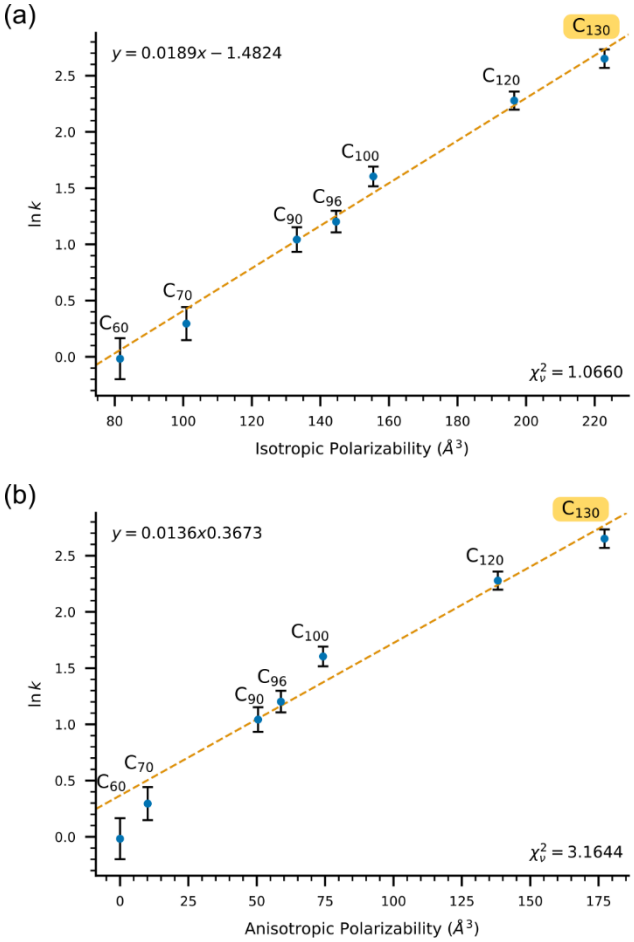

Figure 4. Retention time plots of ln capacity factor (k) versus (a) isotropic polarizability and (b) anisotropic polarizability.

As illustrated in Table 1, HOMO-LUMO gaps for C_{60}-$I_h(1)$, [5,5] C_{70}-$D_{5h}(1)$, [5,5] C_{90}-$D_{5h}(1)$, [5,5] C_{100}-$D_{5d}(1)$, [5,5] C_{120}-$D_{5d}(1)$, and [5,5] C_{130}-$D_{5h}(1)$ range from 1.5-2.7 eV. Oddly, the C_{130}-$D_{5h}(1)$ HOMO-LUMO gap is even higher than C_{120}-$D_{5d}(1)$ and thus predicts a reasonably high isomer stability for C_{130} fullertubes. In contrast, HOMO-LUMO gaps for $D_{5d/5h}$ C_{80}, C_{110}, and C_{140} are predicted to be significantly smaller.[9]

In comparison to C_{60} and C_{70}, Table 1 indicates the [5,5] fullertube family exhibits sufficient solubility in carbon disulfide and aromatic solvents (*e.g.*, *o*-xylene) throughout all phases of purification, *e.g.*, soot extraction, HPLC separation, and UV-vis. A more detailed study with saturation and quantitative solubilities was not feasible for only 50 µg.

Table 1. Overview and comparison of C_{60} and C_{70} fullerenes with [5,5] C_{90}, C_{100}, C_{120} and C_{130} fullertubes.

[5,5] Fullertube Family Member	HOMO -LUMO Gap	Solubility in CS_2 and Aromatic Solvents	Number of Possible IPR Isomers
C_{60}-$I_h(1)$	2.73 eV	Yes	1
C_{70}-$D_{5h}(1)$	2.66 eV	Yes	1
C_{90}-$D_{5h}(1)$	1.93 eV	see Fig. 3e	46
C_{100}-$D_{5d}(1)$	2.18 eV	see Fig. 3e	450
C_{120}-$D_{5d}(1)$	1.45 eV	see Fig. 3e	10,774
C_{130}-$D_{5h}(1)$	1.82 eV	see Fig. 3e	39,393

As a third experimental layer of structural support for [5,5] C_{130}-$D_{5h}(1)$ fullertube, we performed scanning transmission electron microscope (STEM) imaging. Fig. 5a shows an overview of randomly distributed fullertubes imaged on a graphene support. The C_{130}-$D_{5h}(1)$ fullertubes appear identical. Notably, the fullertubes wiggle and move under the influence of the electron beam, sometimes appearing and disappearing at various positions over time. As the C_{130} fullertubes are not deliberately ordered, occasional end-on fullertubes can be seen. In **Fig. 5b**, the background hexagonal pattern is a single layer of graphene. In the lower-right corner, a second layer of graphitized material anchors several [5,5] C_{130}-$D_{5h(1)}$ fullertubes. In the bottom left corner, bright disordered contamination also anchors fullertubes to the graphene support.

Consistent with prior studies of C_{60},[13] imaging with the motion of the fullertubes under the electron beam complicates the direct interpretation of the internal atomic structure. Using background graphene as a reference, we observe an aspect ratio of the fullertube to be consistent with the DFT model for [5,5] C_{130}-$D_{5h}(1)$. As shown in the SI, we further compare the experimental image versus the fullertube structure, C_{130}-$D_{5h}(1)$.

In summary, we overcome decades-long hurdles and false narratives of "too low a yield to isolate pure and pristine higher carbon clusters" and "too many structural isomers to fully separate." Yet, we now report the first experimental and computational characterization of pristine fullertube [5,5] C_{130}-$D_{5h}(1)$, a colossal jump in the number of carbons beyond 100-atoms. As such, this represents the largest soluble all-carbon molecule isolated in purified and pristine form, with isomeric purity, and with the highest aspect ratio to date. With this discovery of C_{130}, the [5,5] fullertube family is extended to *more* tubular carbons (70 atoms) than hemifullerene endcap carbons (30 + 30 atoms, each end). As such, the [5,5] fullertubes cement their place in the lineage of other sp^2 hybridized allotropes of carbon including fullerenes, single-walled carbon nanotubes and nanohorns (SWCNTs and SWCNHs), graphene, and graphite.

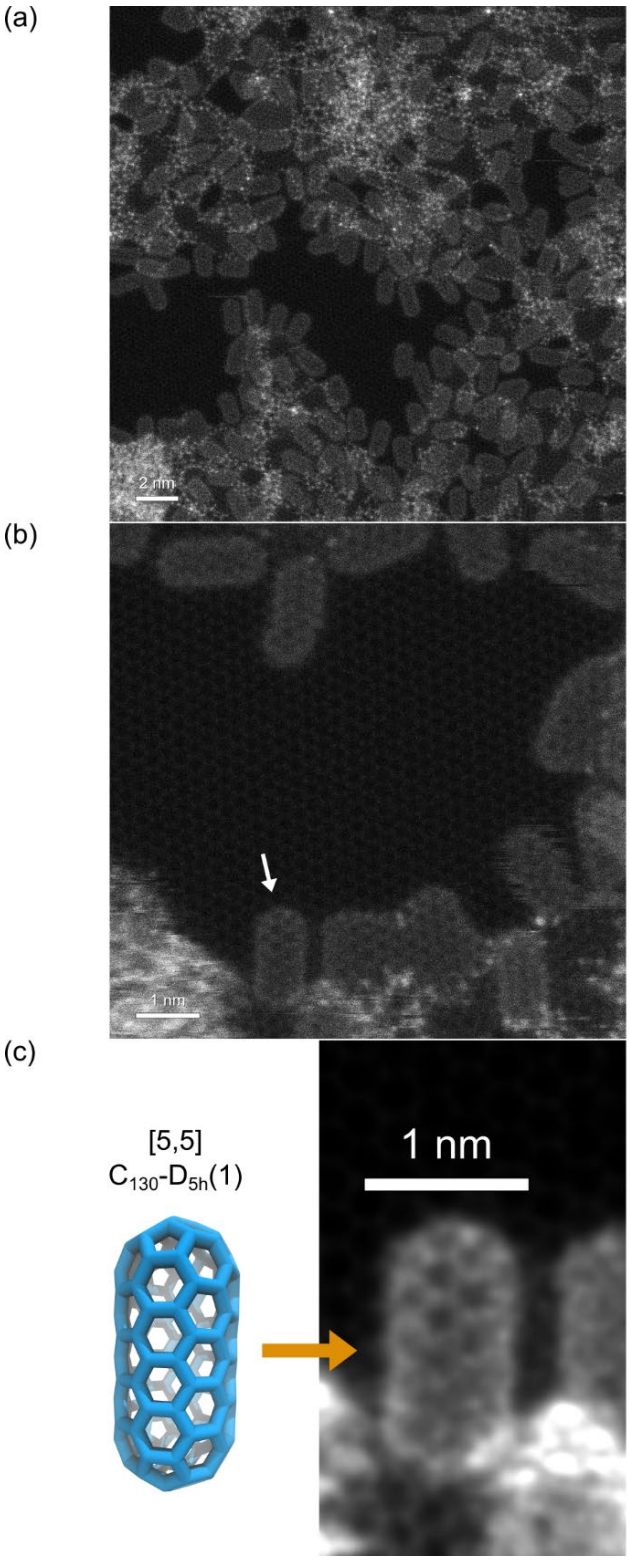

Figure 5. HRTEM images consistent with [5,5] C_{130}-D_{5h}(1) fullertubes show (a) an overview of C_{130} clusters, (b) zoomed in region at the 1 nm scale, and (c) overlay of the C_{130} structure.

ASSOCIATED CONTENT

Supporting Information.

The Supporting Information is available free of charge at https://pubs.acs.org. Experimental details, isolation procedure using aminopropanol and HPLC, DFT theoretical calculations, TEM, and structural information supporting candidate fullertube structures.

AUTHOR INFORMATION

Corresponding Authors

Steven Stevenson – FIRST Molecules Center and Department of Chemistry and Biochemistry, Purdue University Fort Wayne, Fort Wayne, Indiana 46805, United States; orcid.org/0000-0003-3576-4062; Email: stevenss@pfw.edu

Harry C. Dorn – Department of Chemistry, Virginia Tech, Blacksburg, Virginia 24061, United States; orcid.org/0000-0002-3150-5314; Email: hdorn@vt.edu.

Andrew R. Lupini – Center for Nanophase Materials Sciences, Oak Ridge National Laboratory, Oak Ridge, TN 37831, United States; orcid.org/0000-0002-1874-7925; Email: arl1000@ornl.gov.

David B. Geohegan – Center for Nanophase Materials Sciences, Oak Ridge National Laboratory, Oak Ridge, TN 37831, United States; orcid.org/0000-0003-0273-3139; Email: geohegandb@ornl.gov

Authors

Emmanuel Bourret – Département de Physique, Université de Montréal, Complexe des Sciences, 1375 Avenue Thérèse-Lavoie-Roux, Montréal, QC H2V 0B3, Canada ; orcid.org/0000-0001-9856-1794

Xiaoyang Liu – Department of Chemistry, Virginia Tech, Blacksburg, Virginia 24061, United States; orcid.org/0000-0002-2554-3410

Cora A. Noble – Department of Chemistry and Biochemistry, Purdue University Fort Wayne, Fort Wayne, Indiana 46805, United States

Kevin Cover – Department of Chemical Engineering, Virginia Tech, Blacksburg, Virginia 24061, United States

Tanisha P. Davidson – Department of Chemistry and Biochemistry, Purdue University Fort Wayne, Fort Wayne, Indiana 46805, United States

Rong Huang – Department of Chemistry, Virginia Tech, Blacksburg, Virginia 24061, United States

†**Ryan M. Koenig** – Department of Chemistry and Biochemistry, Purdue University Fort Wayne, Fort Wayne, Indiana 46805, United States; orcid.org/0000-0002-7196-3862

K. Shawn Reeves – Center for Nanophase Materials Sciences Oak Ridge National Laboratory, Oak Ridge, TN 37831, United States; orcid.org/0000-0003-4021-9288

Ivan V. Vlassiouk – Center for Nanophase Materials Sciences Oak Ridge National Laboratory, Oak Ridge, TN 37831, United States; orcid.org/0000-0002-5494-0386

Michel Côté – Département de Physique, Université de Montréal, Complexe des Sciences, 1375 Avenue Thérèse-Lavoie-Roux, Montréal, QC H2V 0B3, Canada ; orcid.org/0000-0001-9046-9491

Jeffery S. Baxter – Center for Nanophase Materials Sciences Oak Ridge National Laboratory, Oak Ridge, TN 37831, United States; orcid.org/0000-0002-3786-4190

Present Addresses

†Ryan M. Koenig is currently at the Department of Chemistry, University of California-Irvine, Irvine, CA, 92697, United States

Author Contributions

The manuscript was written through research contributions of all authors. All authors have given approval to the manuscript.

Funding Sources

National Science Foundation: RUI CHE-1856461 and CHE-2247272.

Notes

The authors declare no competing financial interest.

ACKNOWLEDGMENT

SS thanks the Chemistry Division of the National Science Foundation for grants RUI CHE-1856461 and CHE-2247272. H.C.D. thanks Heather Claire Dorn for assistance with Supporting Information figures. Advanced Research Computing at Virginia Tech is gratefully acknowledged for the computational work. Electron microscopy and graphene synthesis and processing conducted as part of a user project at the Center for Nanophase Materials Sciences (CNMS), which is a US Department of Energy, Office of Science User Facility at Oak Ridge National Laboratory and partially supported by the U.S. Department of Energy (DOE), Office of Science, Basic Energy Sciences, Materials Sciences and Engineering Division. This research was financially supported by the Natural Sciences and Engineering Research Council of Canada (NSERC), under the Discovery Grants program Grant No. RGPIN-2016-06666. This research was enabled in part by support provided by Calcul Québec and the Digital Research Alliance of Canada. The operation of the supercomputers used for this research is funded by the Canada Foundation for Innovation (CFI), the Ministère de la Science, de l'Économie et de l'Innovation du Québec (MESI), and the Fonds de recherche du Québec – Nature et technologies (FRQ-NT). E.B. and M.C. are members of the Regroupement québécois sur les matériaux de pointe (RQMP).

ABBREVIATIONS

IPR, isolated pentagon rule; PDA, photodiode array; LDI-TOF, laser desorption ionization - time of flight; HPLC, high performance/pressure liquid chromatography; STEM, scanning transmission electron microscopy.

REFERENCES

(1) Harigaya, K. From C_{60} to a fullerene tube: Systematic analysis of lattice and electronic structures by the extended Su-Schrieffer-Heeger model. *Physical Review B* **1992**, *45* (20), 12071-12076. DOI: 10.1103/PhysRevB.45.12071.

(2) (2a) Ajie, H.; Alvarez, M. M.; Anz, S. J.; Beck, R. D.; Diederich, F.; Fostiropoulos, K.; Huffman, D. R.; Kraetschmer, W.; Rubin, Y.; et al. Characterization of the soluble all-carbon molecules C_{60} and C_{70}. *The Journal of Physical Chemistry* **1990**, *94* (24), 8630-8633. DOI: 10.1021/j100387a004. (2b) Cox, D. M.; Behal, S.; Disko, M.; Gorun, S. M.; Greaney, M.; Hsu, C. S.; Kollin, E. B.; Millar, J.; Robbins, J. Characterization of C_{60} and C_{70} clusters. *Journal of the American Chemical Society* **1991**, *113* (8), 2940-2944. DOI: 10.1021/ja00008a023. (2c) Krätschmer, W.; Lamb, L. D.; Fostiropoulos, K.; Huffman, D. R. Solid C_{60}: a new form of carbon. *Nature* **1990**, *347* (6291), 354-358. DOI: 10.1038/347354a0.

(3) Yang, H.; Beavers, C. M.; Wang, Z.; Jiang, A.; Liu, Z.; Jin, H.; Mercado, B. Q.; Olmstead, M. M.; Balch, A. L. Isolation of a Small Carbon Nanotube: The Surprising Appearance of D_{5h}(1)-C_{90}. *Angewandte Chemie International Edition* **2010**, *49* (5), 886-890. DOI: https://doi.org/10.1002/anie.200906023.

(4) Koenig, R. M.; Tian, H.-R.; Seeler, T. L.; Tepper, K. R.; Franklin, H. M.; Chen, Z.-C.; Xie, S.-Y.; Stevenson, S. Fullertubes: Cylindrical Carbon with Half-Fullerene End-Caps and Tubular Graphene Belts, Their Chemical Enrichment, Crystallography of Pristine C_{90}-D_{5h}(1) and C_{100}-D_{5d}(1) Fullertubes, and Isolation of C_{108}, C_{120}, C_{132}, and C_{156} Cages of Unknown Structures. *Journal of the American Chemical Society* **2020**, *142* (36), 15614-15623. DOI: 10.1021/jacs.0c08529.

(5) Stevenson, S.; Liu, X.; Sublett Jr, D. M.; Koenig, R. M.; Seeler, T. L.; Tepper, K. R.; Franklin, H. M.; Wang, X.; Huang, R.; Feng, X.; et al. Semiconducting and Metallic [5,5] Fullertube Nanowires: Characterization of Pristine D_{5h}(1)-C_{90} and D_{5d}(1)-C_{100}. *J. Am. Chem. Soc.* **2021**, *143* (12), 4593-4599, 10.1021/jacs.0c11357. DOI: 10.1021/jacs.0c11357.

(6) Liu, X.; Bourret, E.; Noble, C. A.; Cover, K.; Koenig, R. M.; Huang, R.; Franklin, H. M.; Feng, X.; Bodnar, R. J.; Zhang, F.; et al. Gigantic C120 Fullertubes: Prediction and Experimental Evidence for Isomerically Purified Metallic [5,5] C_{120}-$D_{5d(}$1) and Nonmetallic [10,0] C_{120}-D_{5h}(10766). *Journal of the American Chemical Society* **2022**, *144* (36), 16287-16291. DOI: 10.1021/jacs.2c06951.

(7) Jover, O.; Martín-Jiménez, A.; Franklin, H. M.; Koenig, R. M.; Martínez, J. I.; Martín, N.; Lauwaet, K.; Miranda, R.; Gallego, J. M.; Stevenson, S.; Otero, R. Nanotube-Like Electronic States in [5,5]-C_{90} Fullertube Molecules. *Small* **2023**, *pending*, in press.

(8) Sanad, M. F.; Franklin, H. M.; Ali, B. A.; Puente Santiago, A. R.; Nair, A. N.; Chava, V. S. N.; Fernandez-Delgado, O.; Allam, N. K.; Stevenson, S.; Sreenivasan, S. T.; Echegoyen, L. Cylindrical C_{96} Fullertubes: A Highly Active Metal-Free O_2-Reduction Electrocatalyst. *Angewandte Chemie International Edition* **2022**, *61* (21), e202116727. DOI: https://doi.org/10.1002/anie.202116727.

(9) Schüßlbauer, C. M.; Krug, M.; Ullrich, T.; Franklin, H. M.; Stevenson, S.; Clark, T.; Guldi, D. M. Exploring the Threshold between Fullerenes and Nanotubes: Characterizing Isomerically Pure, Empty-Caged, and Tubular Fullerenes D_{5h}-C_{90} and D_{5d}-C_{100}. *Journal of the American Chemical Society* **2022**, *144* (24), 10825-10829. DOI: 10.1021/jacs.2c02442.

(10) Fowler, P. W. M. D. E. *An atlas of Fullerenes*; Clarendon, 1995.

(11) Cioslowski, J.; Rao, N.; Moncrieff, D. Electronic Structures and Energetics of [5,5] and [9,0] Single-Walled Carbon Nanotubes. *J. Am. Chem. Soc.* **2002**, *124* (28), 8485-8489, 10.1021/ja0126879. DOI: 10.1021/ja0126879.

(12) (12a) Liu, X. Y.; Zuo, T. M.; Dorn, H. C. Polarizability Effects Dominate the Chromatographic Retention Behavior of Spheroidal and Elipsoidal Metallofullerene Nanospheres.

Journal of Physical Chemistry C **2017**, *121* (7), 4045-4049. DOI: 10.1021/acs.jpcc.6b12558. (12b) Fuchs, D.; Rietschel, H.; Michel, R. H.; Fischer, A.; Weis, P.; Kappes, M. M. Extraction and chromatographic elution behavior of endohedral metallofullerenes: Inferences regarding effective dipole moments. *Journal of Physical Chemistry* **1996**, *100* (2), 725-729. DOI: 10.1021/jp951537f.

(13) Mirzayev, R.; Mustonen, K.; Monazam, M. R. A.; Mittelberger, A.; Pennycook, T. J.; Mangler, C.; Susi, T.; Kotakoski, J.; Meyer, J. C. Buckyball sandwiches. *Science Advances* **2017**, *3* (6), e1700176. DOI: doi:10.1126/sciadv.1700176.